

## **RESISTANCE TO FLOW AND SEDIMENT TRANSPORT IN AGGRADING CHANNELS**

**Elsa Alves**

Research Assistant, Laboratório Nacional de Engenharia Civil  
Av. do Brasil, 101, 1799 Lisboa Codex  
Telephone: ++351 1 8482131; Fax: ++351 1 8473845; e-mail: ealves@lnec.pt  
Portugal

**António H. Cardoso**

Associate Professor, Instituto Superior Técnico  
Av. Rovisco Pais, 1096 Lisboa Codex  
Telephone: ++351 1 8418154; Fax: ++351 1 8497650; e-mail: ahc@civil.ist.utl.pt  
Portugal

### **ABSTRACT**

The purpose of this study is the investigation of resistance to flow and sediment transport in aggrading channels generated by overfeeding. A series of aggradation experiments were carried out by overfeeding sediment load to a movable bed channel previously maintained in equilibrium. The bed and water surface profiles were recorded and the sediment transport rate was measured. These data were used to i) study the time evolution of resistance to flow during the transient situation generated by overfeeding and to ii) check the applicability of the sediment transport model suggested by Yen *et al.* to the observed non-equilibrium sediment transport situation. As a consequence of this analysis, a slightly different version of the model is suggested and a new relation for the calculation of the velocity of the deposition front is proposed.

### **1. INTRODUCTION**

Human activity in alluvial rivers may induce significant changes in their sediment transport capacity; human activity in river basins may cause the change of the sediment load entering a given river cross-section. These changes potentially destroy previously existing equilibrium states, leading to river bed aggradation or degradation.

The case of non-equilibrium flows, where the sediment transport capacity is different from the sediment transport rate is rather more complex than the case of equilibrium (regime) flows. For the equilibrium case, semi-empirical relations regarding the prediction of bed-forms, resistance to flow or sediment transport rate are known at present. Some of these relations produce reliable predictions. However, their reliability decreases for non-equilibrium

(un-balanced) situations induced, e.g., by changes in the sediment transport rate or flow discharge.

Despite of this situation, a comparatively small number of experiments on aggradation or degradation are known at present. Pioneering work was only carried out in the seventies and eighties, namely by SONI (1975) and MEHTA (1980). Thus, it was decided to carry out experiments on aggradation induced by overfeeding. The results of these experiments are presented and discussed in this paper regarding resistance to flow and sediment transport rate.

## 2. EXPERIMENTAL SET-UP, MEASURING EQUIPMENT AND PROCEDURE

The study was carried out in a tilting flume where the water and the sand can be re-circulated simultaneously. The flow entering the flume moves downstream by gravity and then falls into a large downstream sump. From this sump, the mixture of water and sand is pumped through three return pipes into the upstream tank, where a few metallic devices exist to guarantee the flow smoothness and uniformity at the upstream cross-section.

The flume is 40.7 m long and its cross-section is rectangular (2.0 m wide and 1.0 m deep). The flow depth can be controlled by operating two downstream gates. One of this gates is vertical and acts as a thin horizontal-crest weir; the other one is horizontal, slides upstream and downstream at the flume bottom and acts as a bottom outlet. Most of the water is discharged over the vertical gate; the bed load is discharged through the horizontal bottom gate. The flume slope varies between 0% and 2.5%. One extra sand-feeding system, essentially consisting of a big hopper, can be operated at approximately 10 m from the flume entrance cross-section. The overfeeding discharge can be controlled within certain limits.

The measuring equipment comprises one electromagnetic flow-meter per return pipe, one bed-follower probe, one electronic point gauge, the sediment discharge sampling system which intercepts the sand-water mixture below the horizontal gate, and a fixed ruler measuring the vertical displacement of the flume at its downstream end. The bed-follower probe and the electronic point gauge were mounted on a measuring carriage that is driven by a three-phase motor and controlled by a micro-computer. The micro-computer also logs the bed-follower probe and the point gauge, this way allowing the proper reading of the bed profile as well as of the water surface profile.

Two types of experiments were carried out with sand whose granulometric curve is given by  $D_{50} = 0.70$  mm and  $\sigma_D = 1.68$ . The first type of experiments were *equilibrium* (regime) experiments, where the sediment transport capacity was strictly satisfied. The second were *aggradation* experiments, induced by overfeeding. Prior to each equilibrium experiment, the water discharge,  $Q$ , the flow depth,  $h$ , and the bottom slope,  $i_f$ , were set equal to the predictions of regime equations as to guarantee the fast establishment of uniform flow conditions under equilibrium (absence of systematic erosion or deposition). The flow was first sent, slowly, through the upstream end of the flume, this way avoiding the disruption of the sand bed, previously built up flat. Once the flow depth was practically attained, the selected discharge was imposed and the downstream gates were operated as to obtain the right flow depth. Profiling of both the bottom and the water surface were then made at regular time intervals allowing the identification of systematic erosion or deposition along the flume. Flow discharge, water depth and/or flume slope were slightly corrected whenever needed, during the first few hours of each experiment to accelerate the process of reaching equilibrium. The longitudinal profiles also allowed the identification of the onset of completely developed bed-forms. Equilibrium was assumed to be reached when i) the flow was approximately uniform

(bottom slope,  $i_f$ , approximately equal to the slope of the energy grade line,  $J$ ), ii) no systematic erosion or deposition trend was identified, and iii) the bedforms were completely developed. Then, ten profiles (sand bed and water surface) per experiment were measured at time intervals of approximately 15 minutes, and the sediment discharge as well as the water discharge were measured; the time evolution of bedforms, their appearance and vanishing processes were monitored.

Each aggradation experiment started, without any interruption, when the previous equilibrium experiment was completed. The control variables, namely the flow discharge, the opening of the downstream gates and the flume slope, were maintained unchanged from a given equilibrium experiment to the corresponding aggradation experiment; consequently, the initial condition of a given aggradation test was the final condition of the previous equilibrium one. From the beginning of each aggradation experiment the hopper referred to above was operated, the rate of overfeeding being controlled by its opening.

During the aggradation experiments, the same measurements as for the equilibrium experiments were performed; the sediment overfeeding rate as well as the time evolution of the longitudinal position of the deposition front were recorded.

### 3. RESULTS AND DISCUSSION

#### 3.1 Preliminaries

Ten equilibrium experiments (E.1 to E.10) were run. Only six of them were continued as aggradation experiments (S.1 to S.6). For the equilibrium experiments, Table 1 summarises the values of flow discharge,  $Q$ , equilibrium sediment transport rate,  $Q_{se}$ , mean flow depth,  $h$ , average flow velocity,  $U$ , Froude number,  $Fr$ , slope of the energy grade line,  $J$ , and slope of the bottom,  $i_f$ . It also indicates the type of bedforms occurring on the bed. Table 2 summarises, for the aggradation experiments, the duration of overfeeding,  $t$ , the overfeeding transport rate,  $Q_{sa}$ , the final values of the mean water depth, average flow velocity, Froude number, slope of the energy grade line, bottom slope, and type of bedforms. This information was obtained from the aggrading reach only.

Table 1 – Relevant data for the characterisation of the equilibrium experiments

Experiment	$Q$ ( $\text{m}^3/\text{s}$ )	$Q_{se}$ ( $10^{-5}\text{m}^3/\text{s}$ )	$h$ (m)	$U$ (m/s)	$Fr$ (–)	$J$ ( $10^{-3}$ )	$i_f$ ( $10^{-3}$ )	Type of bedforms
E.1	0.230	3.47	0.219	0.356	0.356	1.399	0.889	dunes
E.2	0.180	4.02	0.191	0.342	0.342	1.773	2.303	dunes
E.3	0.160	0.47	0.193	0.299	0.299	0.477	0.739	dunes
E.4	0.160	2.06	0.178	0.340	0.340	1.377	1.221	dunes
E.5	0.160	–	0.246	0.208	0.208	0.210	0.517	flat bed
E.6	0.180	–	0.249	0.231	0.231	0.229	0.364	flat bed
E.7	0.230	9.20	0.198	0.415	0.415	2.584	2.851	dunes
E.8	0.224	4.20	0.226	0.331	0.331	1.194	1.050	dunes
E.9	0.300	4.94	0.246	0.390	0.390	2.445	3.114	dunes
E.10	0.250	3.17	0.237	0.344	0.344	1.724	2.291	dunes

Fig. 1 presents, as an example (experiments E.5 and S.5), the water surface and bottom profiles of both equilibrium and aggradation experiments at the end of each experiment. In this case, where the initial condition of the experiment S.5 was characterised by flat bed with-

out sediment transport, the deposition front moved approximately 7 m downstream, during 463 min (*cf.* Table 2).

Table 2 – Relevant data for the characterisation of the aggradation experiments

Experiment	$t$ (min)	$Q_{sa}$ ( $10^{-5} \text{m}^3/\text{s}$ )	$h$ (m)	$U$ (m/s)	$Fr$ (–)	$J$ ( $10^{-3}$ )	$i_f$ ( $10^{-3}$ )	Type of bedforms
S.1	535	6.96	0.191	0.600	0.438	3.087	8.107	dunes
S.2	430	7.14	0.169	0.531	0.412	2.438	4.001	dunes
S.3	582	7.50	0.160	0.497	0.397	2.023	6.458	dunes
S.4	499	7.35	0.156	0.510	0.412	2.326	5.469	dunes
S.5	463	6.96	0.152	0.524	0.429	2.468	7.800	dunes
S.6	726	6.96	0.201	0.446	0.318	1.689	5.757	dunes

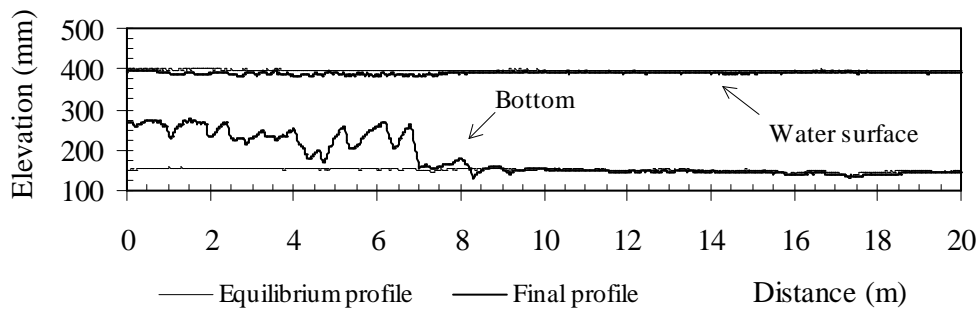


Fig. 1 – Initial and final bed and water surface profiles of experiment S.5.

### 3.2 Resistance to flow

The process of sediment overfeeding was observed to lead to i) the increase of the average bed elevation (aggradation), ii) the change of the bedform dimensions, and iii) the change of the flow depth and velocity. These changes occurred between the overfeeding cross-section (at approximately 10 m from the flume entrance) and the deposition front which moved downstream as the experiment proceeded. This deposition front could be identified with different degrees of precision, the best cases being experiments S.5 and S.6 (*cf.* Fig. 1).

The dimensions of the bedform (dunes) were systematically calculated from the measured bottom profiles. Two validated techniques were used to evaluate the average bottom profiles (trends) for both the equilibrium and the overfeeding tests. The height of the dunes were treated as residuals of the bottom records in respect to such trends. Details of the procedures can be found in ALVES (1997). Fig. 2 shows the time evolution of the wave length,  $\Lambda$ , as well as of the height,  $\Delta$ , of the dunes measured over the deposition reaches of experiments S.1 to S.4. Both  $\Lambda$  and  $\Delta$  are divided by the corresponding equilibrium values,  $\Lambda_e$  and  $\Delta_e$  (experiments E.1 to E.4). Data on experiments S.5 and S.6 were not included because the equilibrium bedforms were flat bed (*cf.* Table 1). From Fig. 2, it can be concluded that with a few exceptions the dimensions of the dunes observed on the deposition reach were smaller than the corresponding equilibrium ones. This variation is more obvious for the wave length; in most cases,  $\Lambda$  and  $\Delta$  increase with time.

*A priori*, the change of the bedform dimensions can be expected to induce changes on resistance to flow. Smaller bedforms might be expected to lead to smaller values of Manning's  $n$ . To test this hypothesis, the values of the Manning coefficient,  $n$ , were back-calculated from the recorded mean flow velocity and mean flow depth. Data obtained on the

deposition reaches were used to calculate the corresponding average  $n$  values. Fig. 3 presents the time evolution of such  $n$  values (experiments S.1 to S.6) as scaled by the values of  $n$  calculated from the corresponding equilibrium experiments,  $n_e$ . From this figure, it is obvious that the  $n$  values of experiments S.5 and S.6 are much higher than the equilibrium values. This result comes to no surprise since the bed for experiments E.5 and E.6 was flat bed. The appearance of bedforms in experiments S.5 and S.6 is obviously responsible for the increase of resistance to flow, i.e., of  $n$ .

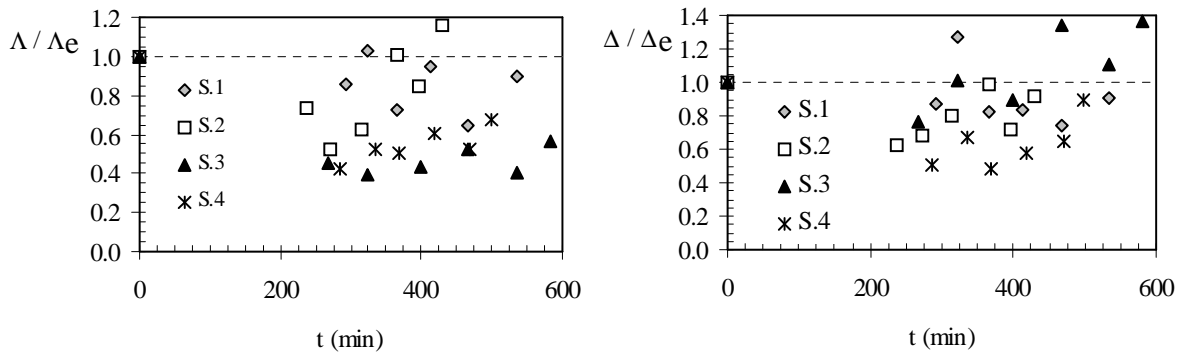


Fig. 2 – Wave length and height of the dunes measured on the deposition reach.

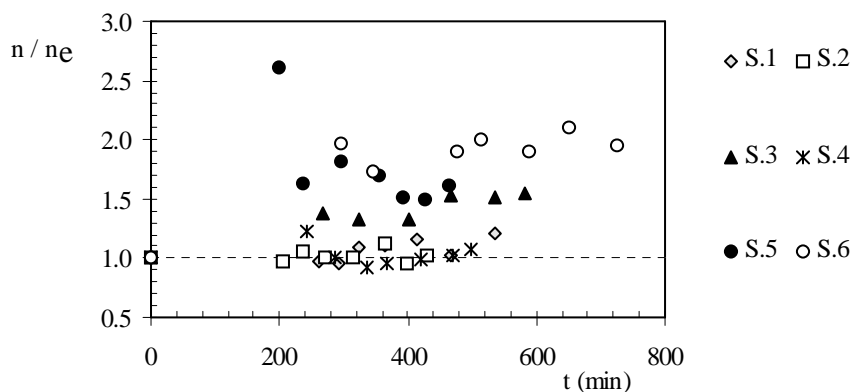


Fig. 3 – Temporal variation of Manning's coefficient.

For the remaining cases, the decrease of the bedform dimensions does not lead to the decrease of resistance to flow, i.e., to the decrease of  $n$ , as expectable. This is particularly true for experiment S.3. However, this fact can be explained as follows. From Fig. 2, experiment S.3, it can be seen that the wave length of the dunes clearly decreases during overfeeding; simultaneously, the height of the dunes remains almost unaltered – in average – as compared with the equilibrium value. This means that the steepness increases. Thus, a bigger number of shorter dunes of roughly unchanged height produces a bigger resistance to flow, which seems realistic. This illustrates that the change of the bedform dimensions by themselves is not enough to characterise the form resistance, namely during transient situations caused by overfeeding. The probable increase of the steepness of the dunes for experiments S1, S2 and S4, would also explain why the resistance to flow does not significantly decrease in these cases either.

### 3.3 Sediment transport

On the basis of the conservation of mass for the sediment phase, YEN *et al.* (1992) suggested the following model which can be used for the prediction of the sediment transport rate of unbalanced sediment transport situations created by overfeeding:

$$Q_s(t) = Q_{se} + Q_{sa} [1 - \exp(-t/t_d)] \quad (1)$$

In this equation,  $Q_s(t)$  is the actual sediment transport rate at a given cross-section,  $Q_{se}$  is the equilibrium sediment transport rate (prior to overfeeding),  $Q_{sa}$  is the overfeeding rate,  $t$  is the time interval counted from the beginning of overfeeding, and  $t_d$  is the time needed for the deposition front to reach the cross-section where the sediment transport rate is evaluated;  $t_d$  can also be seen as the time needed for the bottom of a given cross-section to start its adaptation towards a new equilibrium level. From equation (1), it can be concluded that i) the initial condition, corresponding to  $t = 0$ , is given by  $Q_s(t) = Q_{se}$  along the entire reach, ii)  $Q_s(t) > Q_{se}$  for  $t < t_d$  at any cross-section, and iii)  $Q_s(t) \rightarrow (Q_{se} + Q_{sa})$  as  $t \rightarrow \infty$ .

Conclusion ii) means that, once overfeeding starts, the sediment transport rate at a given cross-section would immediately start increasing, even for  $t < t_d$ . This conclusion does not seem realistic since the sediment particles will always take some time to move from the overfeeding cross-section to any other cross-section situated downstream. This fact could be confirmed from the experiments. Thus, the model suggested by Yen *et al.* was slightly modified and written as follows:

$$Q_s(t) = Q_{se} \quad \text{for } t \leq t_d \quad (2)$$

$$Q_s(t) = Q_{se} + Q_{sa} \left[ 1 - \exp\left(-\frac{t-t_d}{t_d}\right) \right] \quad \text{for } t > t_d \quad (3)$$

where  $t_d$  corresponding to a given position  $x$  is given by  $t_d = x/U_w$  and  $U_w$  is the velocity of the deposition front.

The time evolution of the sediment transport rate along the deposition reach was analysed on the basis of the previous models. This analysis required the calculation of the sediment transport rate at a number of cross-sections and for some time instants. The calculations were performed by using successive records of the bottom profile and applying the continuity equation of the sediments, approached by

$$Q_{s_{i+1}} = Q_{s_i} - \frac{B\Delta y\Delta x}{\Delta t} \quad (4)$$

In this equation, written for a given  $t$ ,  $Q_{s_i}$  and  $Q_{s_{i+1}}$  refer to the sediment transport rate by volume at two consecutive cross-section,  $B$  is the bottom width,  $\Delta x$  is the distance between section  $i$  and section  $i+1$ , and  $\Delta y$  is the variation in the bed elevation occurred in the time interval,  $\Delta t$ .

Fig. 4 shows the time evolution of the sediment transport rate calculated with equation 4 for sections  $x = 1,0$  m,  $x = 2,0$  m ... and  $x = 6,0$  m, experiment S.3. In this experiment,  $Q_{sa} \gg Q_{se}$  ( $Q_{sa}/Q_{se} \approx 16$ , cf. Tables 1 and 2). Fig. 4 shows that the sediment transport rate, at a given cross-section, starts increasing towards a new equilibrium state when the deposition front reaches it, the final (equilibrium) transport rate asymptotically being  $Q_{se} + Q_{sa}$ . This asymptote is approached earlier at the cross-sections nearer to the overfeeding section than further downstream.

Fig. 4 also shows the results of the application of the model of Yen *et al.* (equation 1) as well as of its modified version (equations 2 and 3) to the same data. Keeping in mind the scatter usually found in sediment transport related problems, Fig. 4 could be argued to indicate that both models follow the data reasonably well. However, it is physically incongruent to accept that, at a given cross-section,  $Q_s(t) > Q_{se}$  for  $t < t_d$ . On the other hand, it seems obvious that the deviations between the actual sediment transport rate and the predictions of the model of Yen *et al.* become more important for small  $t$  as the distance to the overfeeding point,  $x$ , increases. These deviations do not exist for the modified version suggested in this paper.

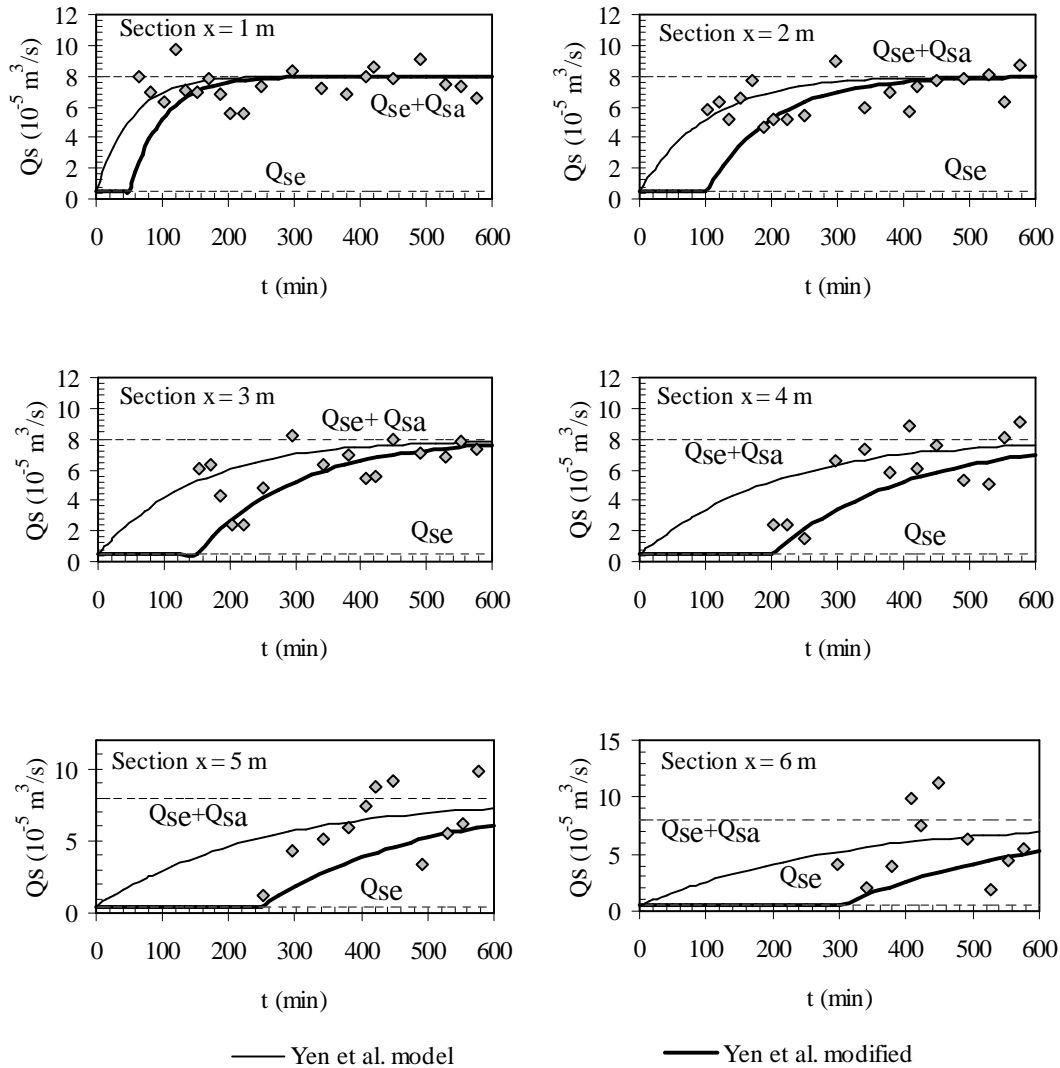


Fig. 4 – Time and space evolution of sediment transport rate for experiment S.3.

From above, it can be concluded that the modified version of the model of Yen *et al.* properly describes the sediment transport phenomenon along a deposition reach, both in space and time, if we know i) the sediment transport rate of the previous equilibrium state, ii) the overfeeding sediment transport rate and iii) the velocity of the deposition front,  $U_w$ . Thus,  $U_w$  is a crucial variable.

In this study,  $U_w$  was calculated from the successive positions which the deposition front occupied along time. The same procedure was applied to the data of SONI (1975).

Through the application of multiple regression to these data as well as to the data published by YEN *et al.* (1992) the following equation was established

$$\frac{U_w}{\sqrt{gD_{50}}} = 10^{3.19} i_f^{1.65} \left( \frac{Q_{sa}}{Q_{se}} \right)^{0.2} \sigma_D^{-2.74} \quad (5)$$

This equation gives  $U_w$  as a function of the median diameter of the bed material,  $D_{50}$ , equilibrium bottom slope,  $i_f$ , sediment transport rates,  $Q_{se}$  and  $Q_{sa}$ , and gradation coefficient of the bed material,  $\sigma_D$ . The above equation is significantly different from the one suggested by Yen *et al.* However equation (5) is believed to be the most adequate of them since it was obtained from a bigger set of equally reliable data.

#### 4. CONCLUSIONS

From the discussion on the influence of overfeeding on the time evolution of resistance to flow and sediment transport along a movable-bed reach, the following results were established:

- The observed decrease of the dimensions of the dunes does not necessarily imply the concomitant decrease of the coefficient  $n$  of Manning during the transient flows generated by overfeeding and presumably leading to a latter equilibrium situation.
- At a given cross-section, once this cross-section is reached by the deposition front, the sediment transport discharge suddenly increases a very fast rate; then it tends asymptotically to the sum of the equilibrium sediment transport rate and the overfeeding sediment transport rate.
- At a given cross-section, the velocity of the deposition front plays a crucial role on the time evolution of flow properties such as the sediment transport rate or the bottom level.
- The velocity of the deposition front was established as a function of the median diameter of the bed material, the equilibrium bottom slope, the equilibrium and the overfeeding sediment transport rates, and the gradation coefficient of the bed material.
- The model of Yen *et al.* was slightly modified as to properly predict the time evolution of sediment transport rate along the deposition reach.

#### REFERENCES

- ALVES, E. – *Estudo experimental de escoamentos em desequilíbrio em canais com leito móvel. O caso da deposição.* (in Portuguese). M. Sc. Thesis, Instituto Superior Técnico, Lisboa, Portugal, 1997.
- MEHTA, P. J. – *Study of aggradation in alluvial streams.* Ph.D. Thesis, University of Roorkee, India, 1980.
- SONI, J. P. – *Aggradation in streams due to increase in sediment load.* Ph.D. Thesis, University of Roorkee, India, 1975.
- YEN, C.; CHANG, S.; LEE, H – *Aggradation – degradation process in alluvial channels.* Journal of Hydraulic Engineering, ASCE, vol. 118, No. 12, December 1992, p. 1651–1699.